Setup for Precise Measurements of beta-decay in Optically Trapped Radioactive Na

Sohani, Moslem

Chapter 5

Recoil-ion Detector

The daughter nucleus gains in a β-decay a rather small energy which is determined by the momentum balance with the lepton pair and its relatively large mass. In a three-body decay, the energies of the recoil-ion and the leptons are broad distributions. After a β^+-decay the daughter atom is left with one too many electron in the atomic shell relative to the charge of the nuclei unless secondary processes after the decay leave the daughter system neutral or ionized. If the system is born negatively charged, the extra electron is very loosely bound. Due to the recoil momentum of the nucleus after the decay, the electron shell feels a shock move that may shake off one or more electrons. The shake off effect can lead to different charge states of the daughter atom. The β^--decay leads to a positively charged ion to start with and the shake off process may increase the charge state afterwards. The energetic ion after the β-decay is called recoil-ion.

In this chapter the principles and design of a reaction microscope for low energy recoil-ion detection are explained. The details of the actual setup and the results from the test measurements are presented.

5.1 MOT-RIMS

Recoil-ion momentum spectroscopy was developed in the 1990's to measure low energy ions emitted in molecular dissociation processes [Ull97]. This technique is based on COLTRIMS (COLd Target recoil-ion Momentum Spectroscopy) with the coincident detection of an electron or photon. The energy of the ions in molecule breakup are of order eV. Therefore the ion's energy distribution is distorted by interaction with molecules at thermal energy. Hence the sample should be cooled to a low temperature without substrate. COLTRIMS started with the

invention of supersonic atomic jets. These produce cold atomic beams by fast expansion and leads to a temperature as low as 15 K [Mer95]. Later atomic traps provided cold samples down to mK temperatures [Wol00]. In a MOT-RIMS setup the MOT cloud containing trapped atoms is located at the center of the RIMS detection system. Ions coming out of the trap are accelerated and guided in an electric field and projected on a MCP detector. This allows for a 4π detection for the ions. At this higher energy the ions have also a higher detection efficiency on the MCP. This detection efficiency for ions of keV kinetic energy is at the level of 20-50% depending on the energy and the impact angle of the ion. MCP detectors can detect neutral atoms too. The detection efficiency for the neutrals is smaller than for ions. Moreover they are not affected by the electric field and the detection coverage is limited by the geometrical solid angle of the MCP as seen from the MOT position.

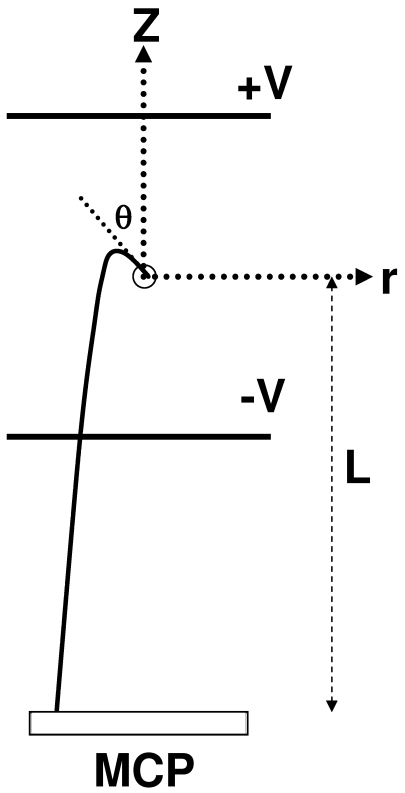

FIG. 5.1: Coordinates of the recoil-ion spectrometer. The start angle θ is defined as the angle between the z axis and the original recoil-ion momentum. Because of the cylindrical symmetry only the radial space coordinate r perpendicular to z matters.

5.1.1 Ion Kinematics in RIMS

Ions in the electric field follow a ballistic trajectory towards the MCP. The situation is similar to a ballistic trajectory in a gravitational field. An ion hits the MCP at a position (x, y) after a time T of flight (TOF). Since the decay products are emitted in a plane (Sec. 2.6) we can translate the coordinate of the hit to the distance from the center ($r = \sqrt{x^2 + y^2}$) and T. If we assume that the electric field is constant all over the path, one can connect the r and T to the initial momentum of the ion.

$$\begin{aligned} p_r &= Mv_r = Mr/T, \\ T &= (v_z + \sqrt{v_z^2 + 2a'L})/a', \\ p_z &= \frac{M(-2L + a'T^2)}{2T}, \\ p_{re} &= \sqrt{p_z^2 + p_r^2}, \\ a' &= E_f q/M, \end{aligned} \tag{5.1}$$

where L is the distance between the starting point of the motion and the MCP, E_f is the electric field, M is the mass of the ion, q is the charge of the ion, v_r and v_z are elements of the initial velocity of the ion, a' is the acceleration of the ion and p_{re} is the total momentum of the recoil-ion. In this derivation the recoil-ion can be treated classically due to its low energy.

The size of the MOT cloud is typically a few millimeters. This means that the path length L, which is typically 10 cm, is not equal for all the events. Their TOF will be different since the initial coordinates r and z are not always zero. This contributes to the resolution of the momentum spectrometer. The position of a hit on the MCP and its TOF are connected through:

$$\begin{aligned} r &= r_0 + v_r T, \\ T &= (v_z + \sqrt{v_z^2 + 2a'L'})/a', \\ L' &= L + z_0, \\ v &= \sqrt{2E_{re}/M}, \\ v_r &= v * \sin\theta, \\ v_z &= v * \cos\theta, \end{aligned} \tag{5.2}$$

where r_0 and z_0 are the initial position coordinates of the recoil-ion, θ is the azimuthal angle of the recoil-ion momentum relative to the z axis (see Fig. 5.1) and E_{re} is the energy of the recoil-ion. Figure 5.2(c) shows the effect of the size of the MOT cloud on position and TOF of an event.

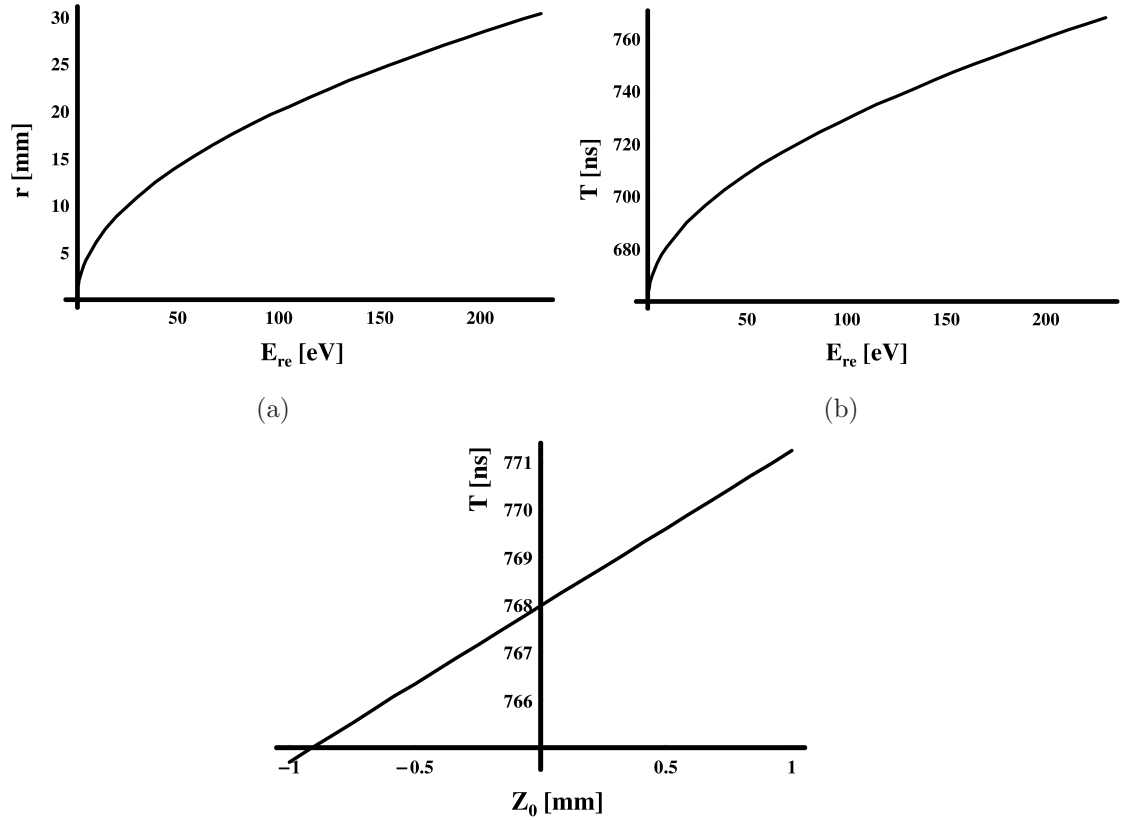

FIG. 5.2: a) Radial position of the ion hit on the MCP for the spectrum of recoil-ion energies when θ=90. b) The TOF of ions (T) for different energies at $\theta = 0$. c) Effect of the initial position on the TOF of ions (T) for $E_r = 230$ and $\theta = 0$. The electric field is 1 kV/cm.

5.1.2 Recoil-Ion Spectra

The MOT cloud size influence on the radial position and on the TOF can be compensated with electrostatic lenses. This technique is known as space focusing or time focusing. Unfortunately it is not possible to achieve both focusing effects simultaneously, because they counteract each other.

Figure 5.2(a) and 5.2(b) show the range of the values for r and T of ^{21}Ne recoil ions in an electric field of 1 kV/cm. The maximum value of r is reached at $\theta \simeq 82^{\circ}$ (see Fig. 5.3). This causes an overlap of the positions for ions with different energies and angles. The ambiguity in position can be resolved using the TOF information.

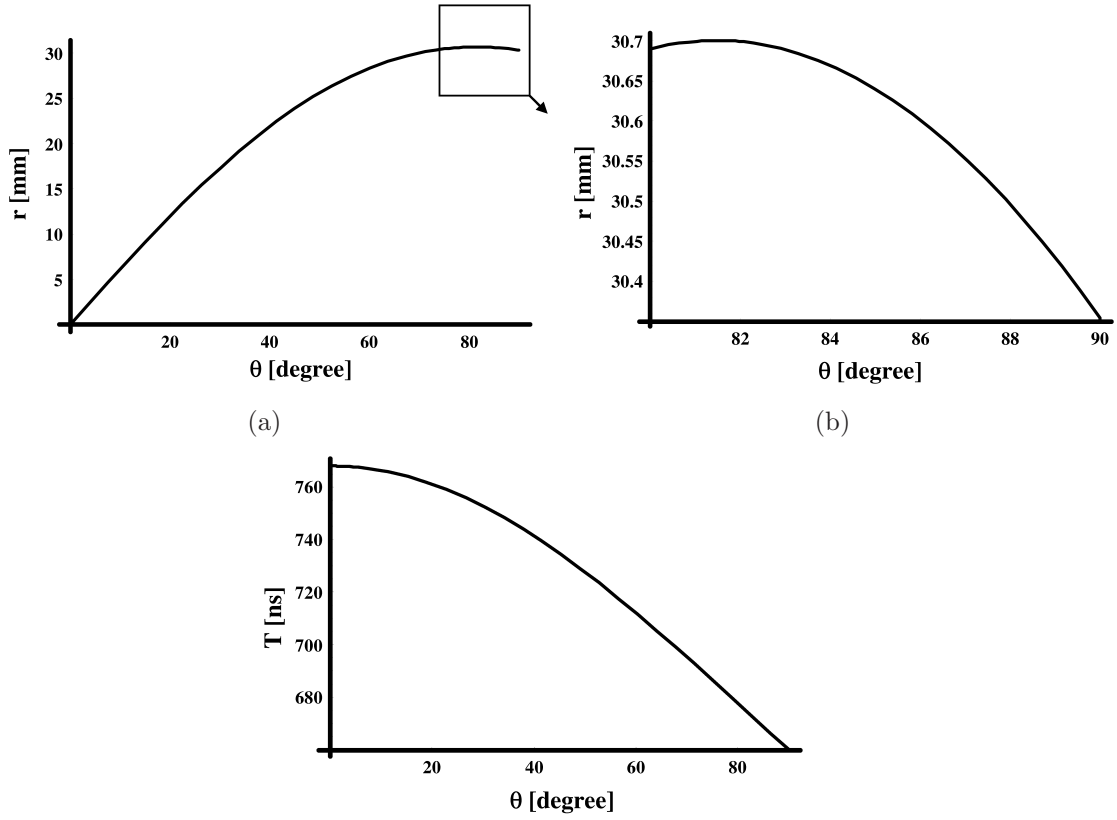

FIG. 5.3: a,b) Radial position of the ion hit on the MCP for different angles (θ) when $E_r = 230eV$. c) TOF for the same energy and different angles (θ).

The recoil-ion momentum is measured in the RIMS setup in terms of the TOF and the position on the MCP detector. Considering the fact that β-decay occurs in a plane, the distance r at which the ion hits on the MCP from its center defines one of the momentum coordinates p_r. Together with the TOF the second component p_z can be obtained. Therefore one can reconstruct the recoil-ion momentum in terms of r and T

$$\begin{aligned} E_{re} &= M * v_r^2/2c^2, \\ v_{re} &= \sqrt{v_r^2 + v_z^2}, \\ v_r &= r/T, \\ v_z &= (a'T^2/2 - L)/T. \end{aligned} \tag{5.3}$$

This allows to determine the event distribution of ^{21}Ne β-decay as a function of the radial coordinate r of the ion impact position on the MCP and the TOF of the recoil-ion (see Fig. 5.4). Figure 5.4(d) shows the effect of a 1% change

in the coefficient "a" in equation A.18 relative to its SM value on the recoil-ion spectrum.

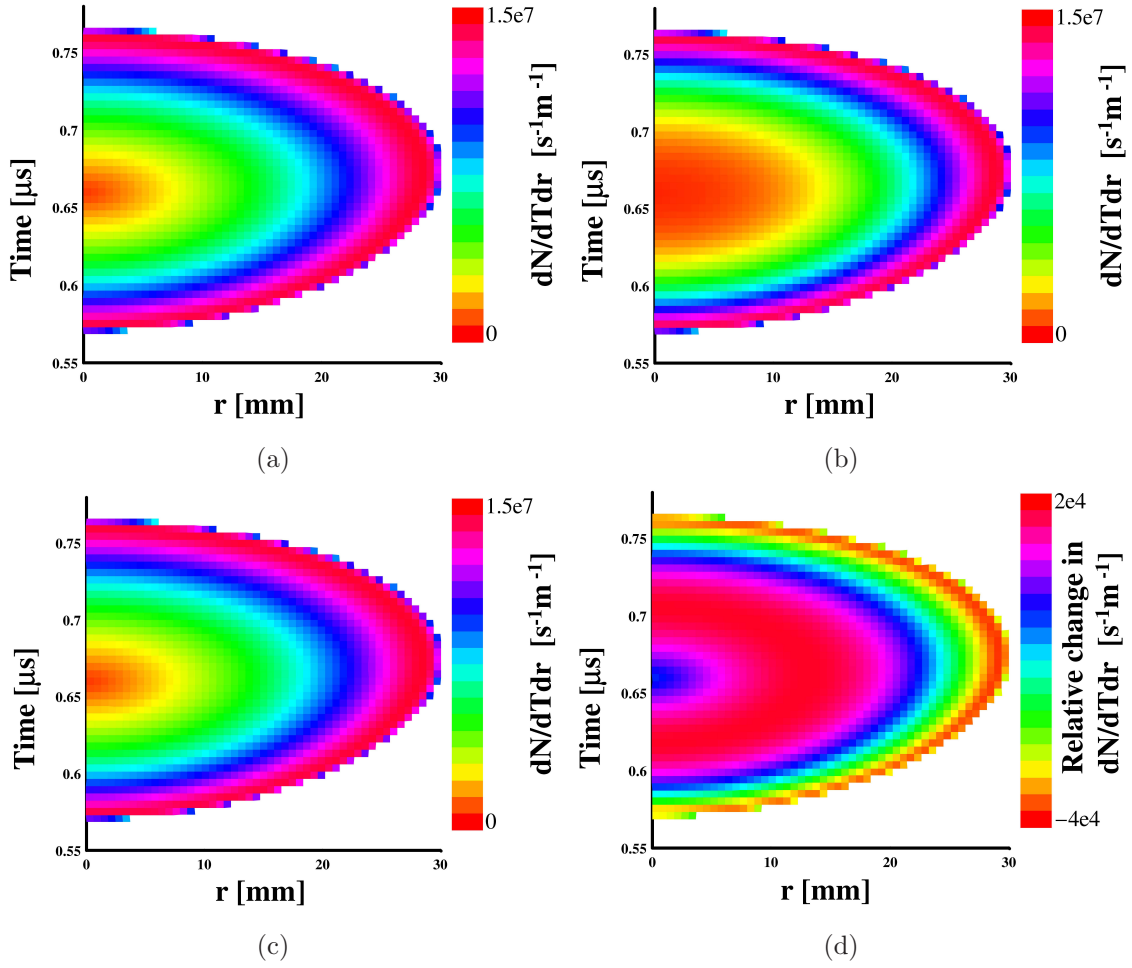

FIG. 5.4: The event distribution of ^{21}Na β-decay in terms of the ion impact radial position r and the TOF T, (a) for a=0, (b) for a=1 and (c) for a=0.588 in the ^{21}Na decay. (d) A 1% change in the SM value of coefficient "a" for ^{21}Na causes a difference in the spectrum (d).

5.2 Design of the Reaction Microscope

The recoil-ion spectrometer in the detection chamber (see Fig. 5.5 and 5.6) consists of a set of electrodes to provide a homogenous electric field in the MOT region and MCP detector with 3 plates in "Z" configuration. An ion hitting the front of the MCP detector creates secondary electrons which are amplified in the

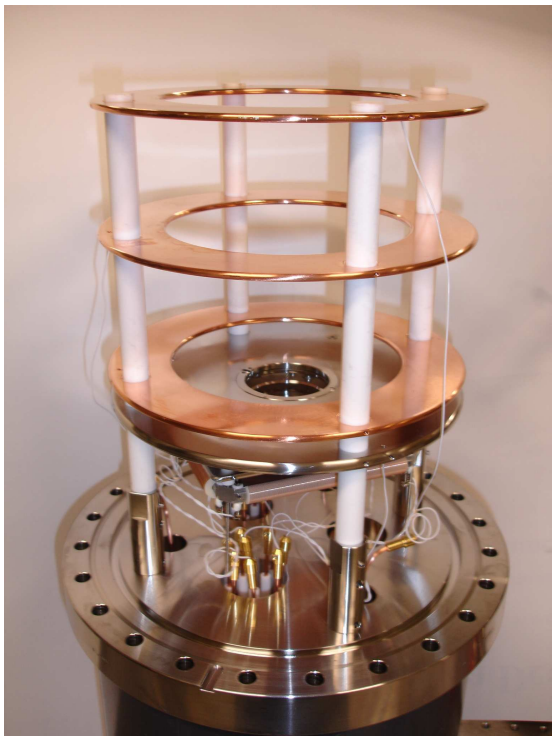

(a)

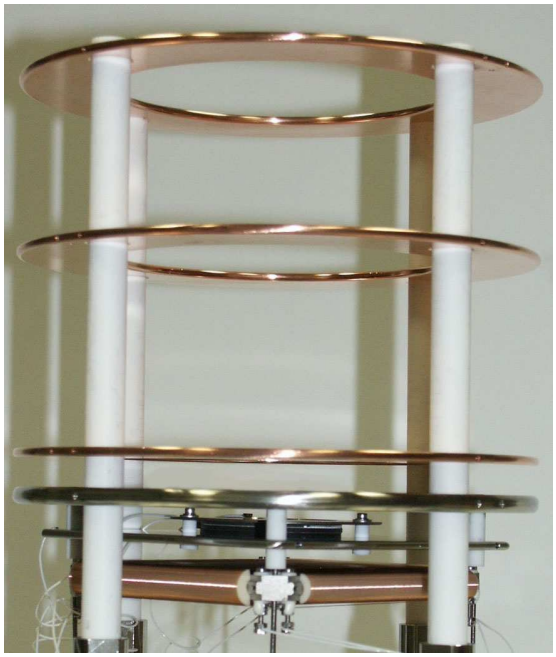

(b)

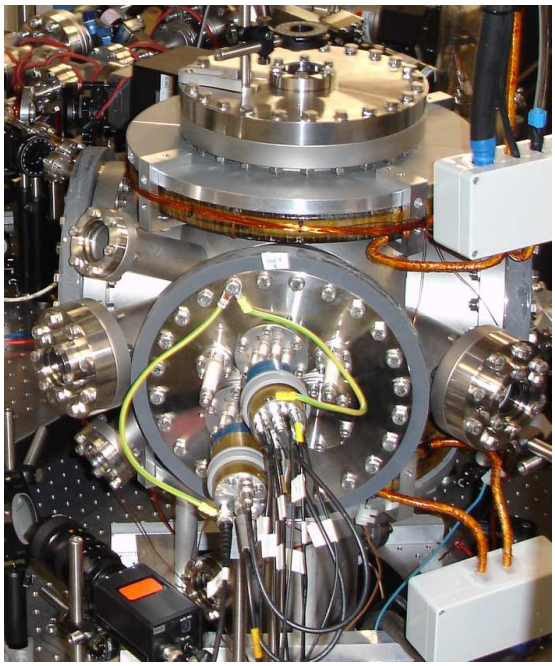

(c)

Fig. 5.5: Recoil-ion momentum spectrometer. a) Copper rings serve as electric field shaping electrodes. The location of the MOT is in the center of the top two electrode rings. b) The Z-stack MCP detector with delay line anode is at the back of the setup. c) Read out at the air side is achieved by UHV feedthroughs to which every single electrode is connected. The resistor and capacitor output coupling network is mounted directly with a socket to the connectors of the multiple feedthrough.

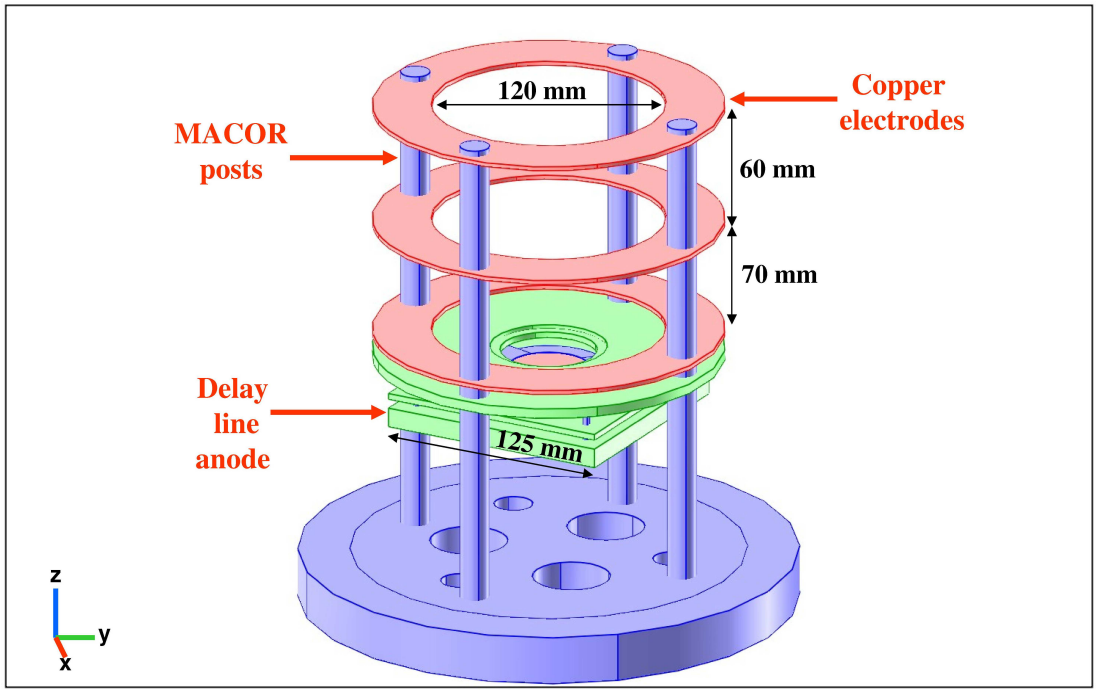

(a)

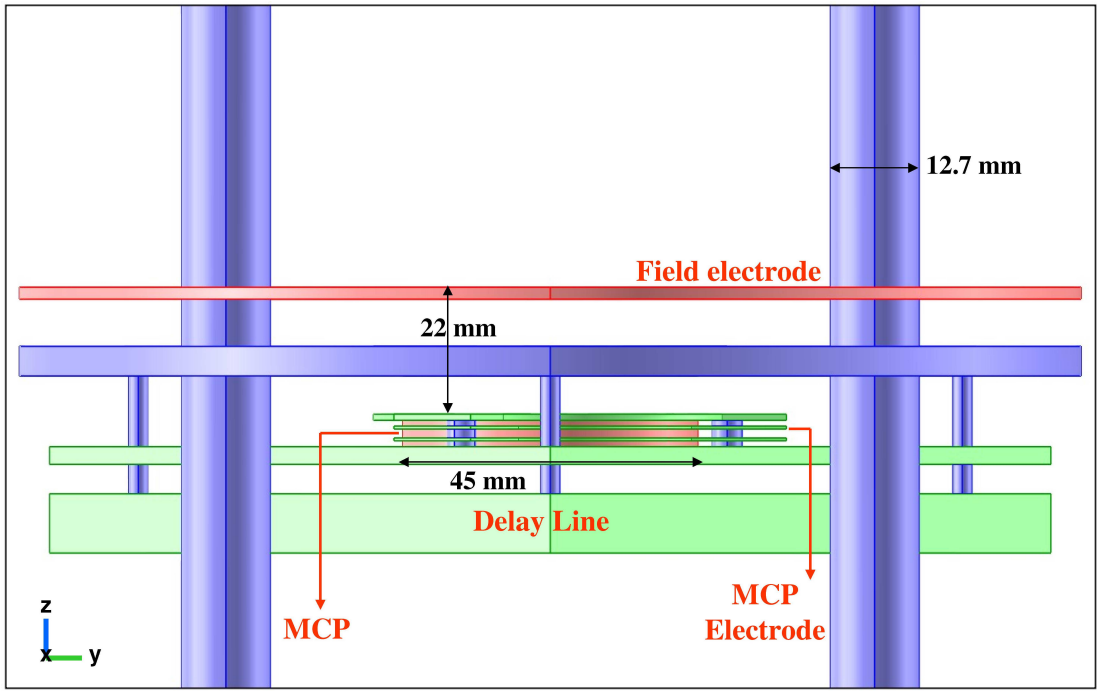

(b)

FIG. 5.6: a) Assembly of the TRIμP recoil-ion momentum spectrometer. b) Details of the MCP detector in the reaction microscope. It is a stack of 3 plates in "Z" configuration.

channels of the plates. A two dimensional delay line anode at the back of the MCP stack collects charge pulses and provides position information. The electric field projects all recoil ions onto the MCP detector. The front plane of the MCP assembly is kept at ground potential. The electrodes are at positive voltages of order 10 kV. The back side of the MCP and the delay line anode are at positive voltages to amplify and collect the electron pulses.

The delay line is made of two pairs of wires wound on a 125 mm×125 mm frame in orthogonal direction (x and y) which has an active area of 80 mm×80 mm (RoentDek DLD80). The wire spooling is 1 mm. The total length of each wire corresponds to 13 Ω resistance. 80 windings in each direction allow a position resolution of better than 1 mm. Wires in each direction are insulated from each other. One of the two wires is on a 300 Volt higher potential to focus and collect the charges which then form an electron pulse. This wire is called signal wire and the other one is the reference wire. Both wires have mostly the same noise through electric pickup. The wires are read at both ends via capacitive coupling. The signals from both ends of each two wire pairs are amplified in 2 GHz amplifiers and fed into a differential amplifier which are all mounted in a four channel NIM module (see Fig. 5.9). In this way, common noise on the wires is eliminated and a clear signal is amplified in the electronic circuit shown in figure 5.10. The time difference between two pulses from the two ends of the same wire can be used to find back the position of the corresponding hit on the detector (see Fig. 5.8).

A signal derived from the break down of the voltage across the MCP high voltage resistive divider provides the reference for the timing measurements. Therefore the position in the directions x and y are

$$\begin{aligned} x &= x_0 + (t_{x1} - t_{x2})d/2. \quad \text{and} \\ y &= y_0 + (t_{y1} - t_{y2})d/2, \end{aligned} \tag{5.4}$$

where x and y are the coordinates of an event and d is the signal propagation speed along one direction on the delay line. It is 0.51 mm/ns for this type of delay lines. The time coordinates t_{x1}, t_{x2}, t_{y1} and t_{y2} are the time differences of signals from both ends of both wire planes. They are in the experiment measured relative to the timing signal derived from the voltage breakdown across the voltage divider supplying voltages to the faces of the plates in the MCP (see Fig. 5.7(a)). The coordinates x_0 and y_0 give the position of the MCP center.

In the present setup we have a 80 mm square delay-line while the diameter of the MCP plates is 40 mm. This is sufficient to collect all the recoil-ions from ^{21}Na decay on the MCP detector using E_f=1 kV/cm electric field (see Fig. 5.2(a)).

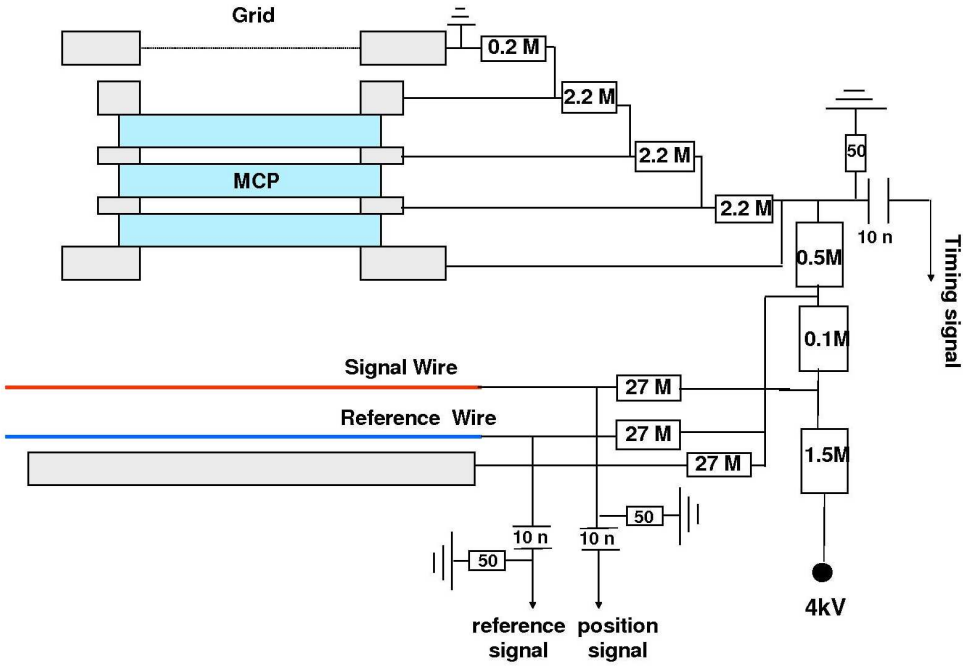

(a)

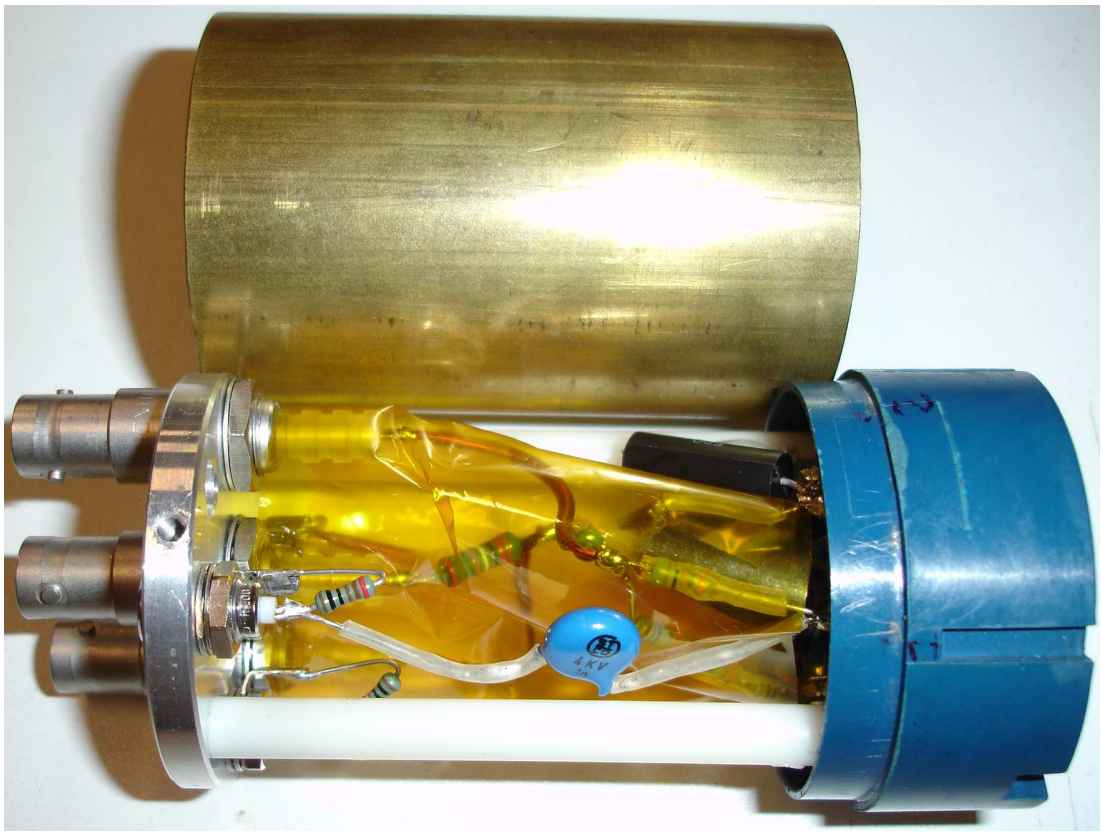

(b)

FIG. 5.7: a) Schematics of the MCP and delay-line anode voltage divider. b) The actual voltage divider socket can be plugged on the power UHV feedthroughs.

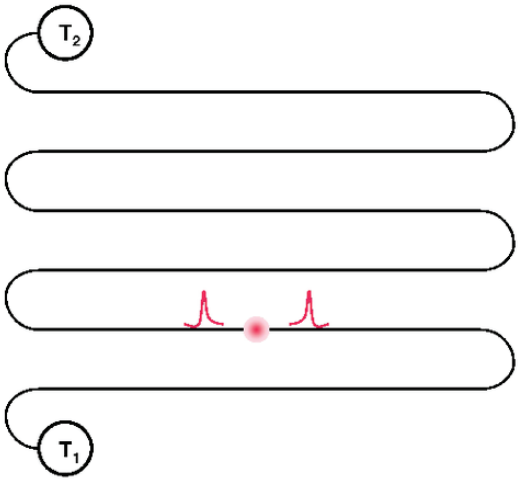

Fig. 5.8: Pulse propagation along a delay line anode wire. The position of an electron shower can be found using the arrival time difference between two pulses at both ends of the wire.

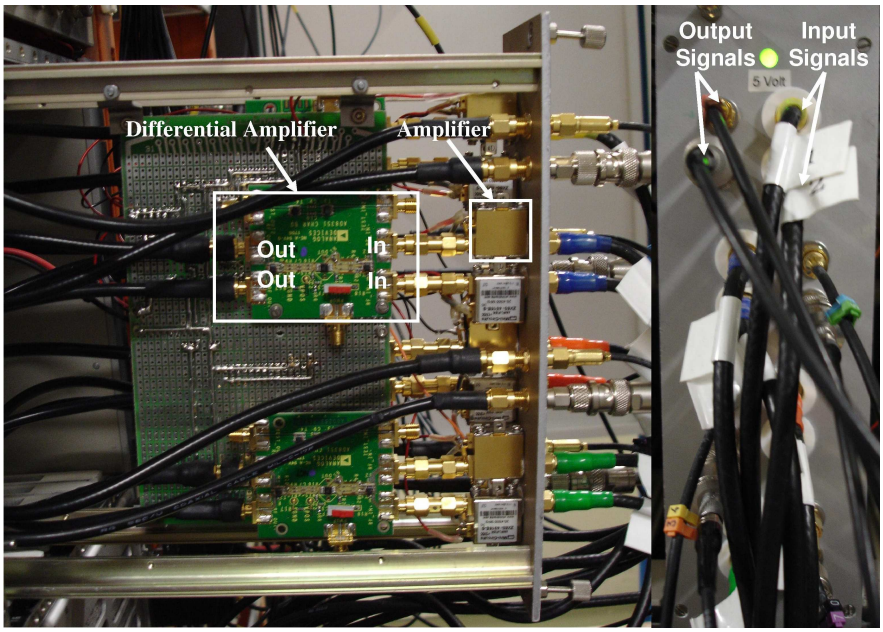

Fig. 5.9: Four channel differential amplifier NIM module which amplifies the MCP signal on the 2-D delay line anode. The signals from all four ends of a pair of signal and reference wires are amplified each in 20 MHz- 3 GHz amplifiers (Mini circuits model ZX60-3018G+) and fed into a differential amplifier (Analog Devices model AD8351). Two independent output signals are available per wire end at the front panel.

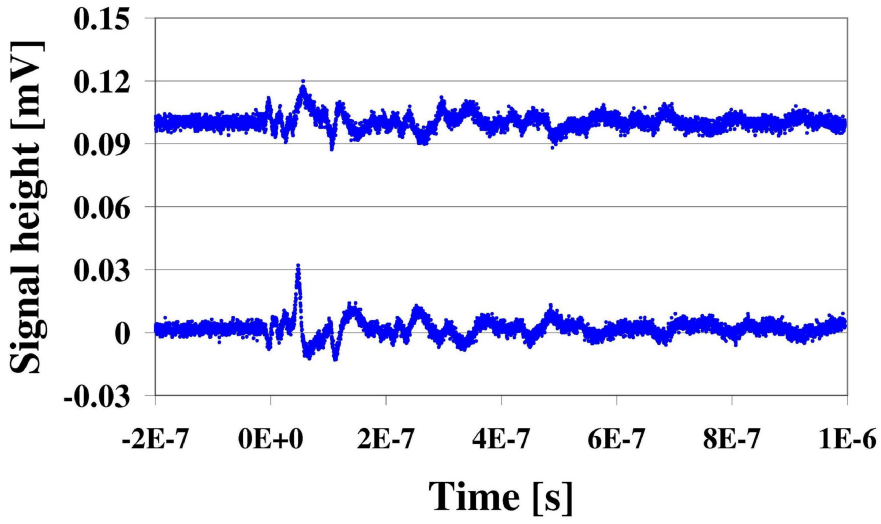

(a)

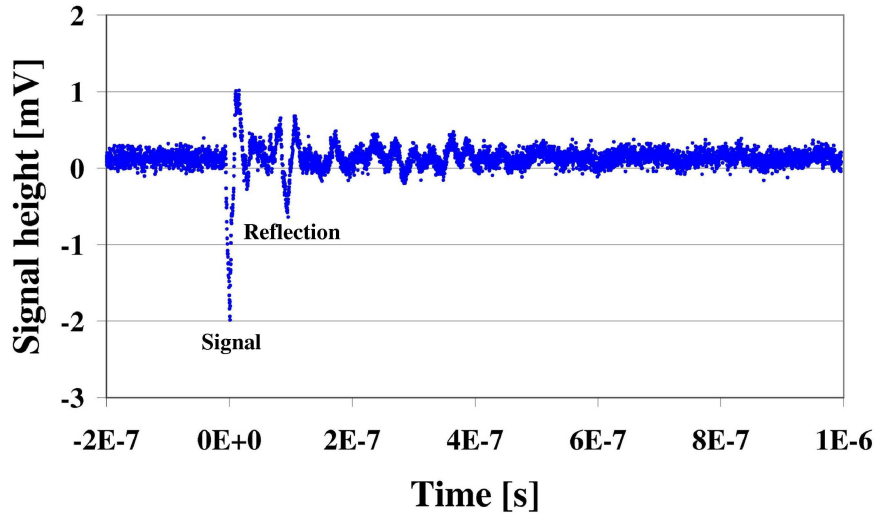

(b)

FIG. 5.10: a) Delay line anode signals of the reference wire (upper trace) and the signal wire (lower trace). b) Differentially amplified signal displayed with a 1 GHz oscilloscope. The second visible pulse is caused by a reflection at the opposite side of the delay line. It is due to the unavoidable impedance mismatch in the vacuum feedthroughs.

The setup has provision for larger diameter MCP plates up to 80 mm diameter to increase resolution at a future stage.

5.3 Field and Ion Guide Simulations

The electric and magnetic fields in the setup (see Fig. 5.11 and 5.12) have been simulated using the COMSOL software package. It is based on finite element calculations in three dimensions and uses various numerical approaches to find the physical parameters.

Distortion caused by the MACOR posts supporting the field shaping electrodes causes a small electric field asymmetry especially close to the copper rings which are the main electrodes (see Fig. 5.11(a)). This effect distorts ion trajectories from their simple ballistic motion. Also the distance between the rings causes curved equipotential surfaces and has a lensing effect on the ion motion (see Fig. 5.11(b)). The trajectories of the recoil-ions can be traced in the same simulation program (see Fig. 5.13). They are distorted by the presence of the electrodes and their support material. The MOT magnetic field in the detection chamber is shown in figure 5.12. Since the magnetic field is almost parallel to the velocity vector of the recoil-ion, the Lorentz force is not large. The imperfections in the electric and magnetic fields need to be taken in to account in the data analysis when the actual ion trajectories are searched.

5.4 Tests and Calibrations

The ion position dependence of the MCP response and the local distortions of the electric field are specific to each particular reaction microscope. A straightforward way to gain control over these effects is to calibrate the detector and measure the response of the MCP for different recoil-ion energies and different initial positions. The initial tests and measurements are done within the scope of this thesis while further calibration test are planned to be done.

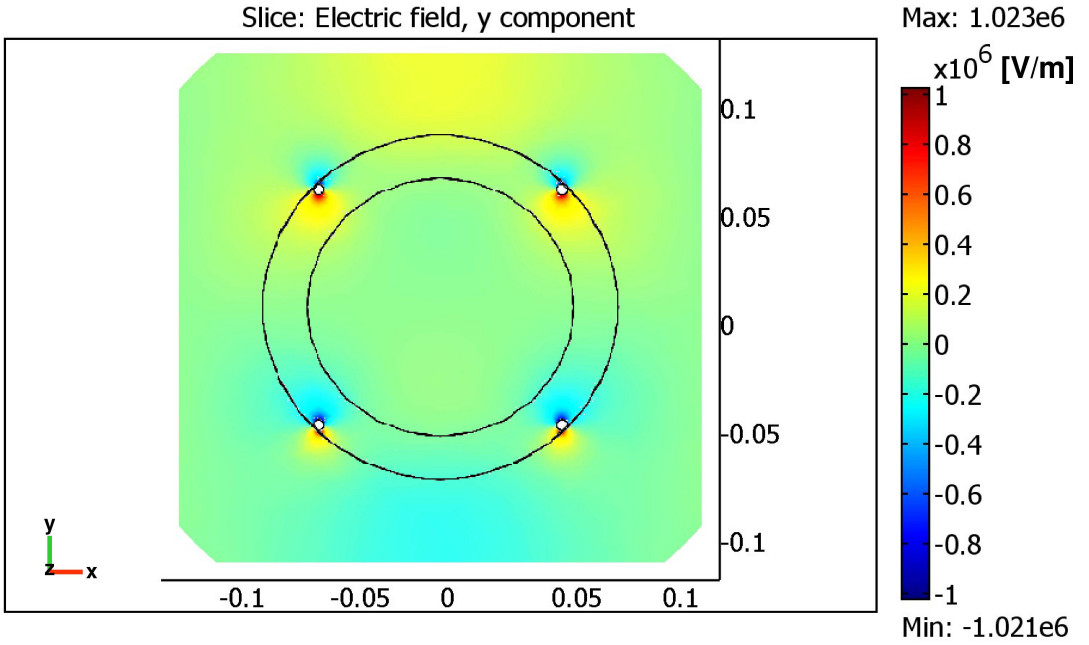

(a)

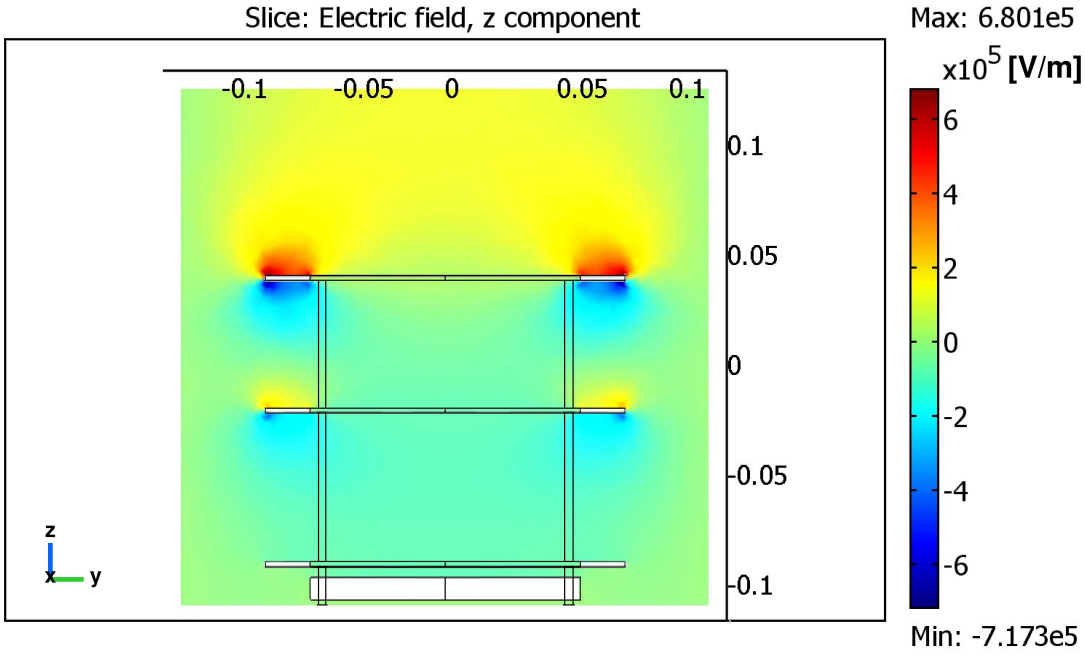

(b)

FIG. 5.11: Calculated electric field in the vicinity of the detection MOT obtained with the program package COMSOL. (a) The MACOR posts distort the x and y component of the electric field. Here the y component is shown for z=0. (b) The electric field shaping rings can form an electric lens, depending on their distance. Here the z component is shown for x=0.

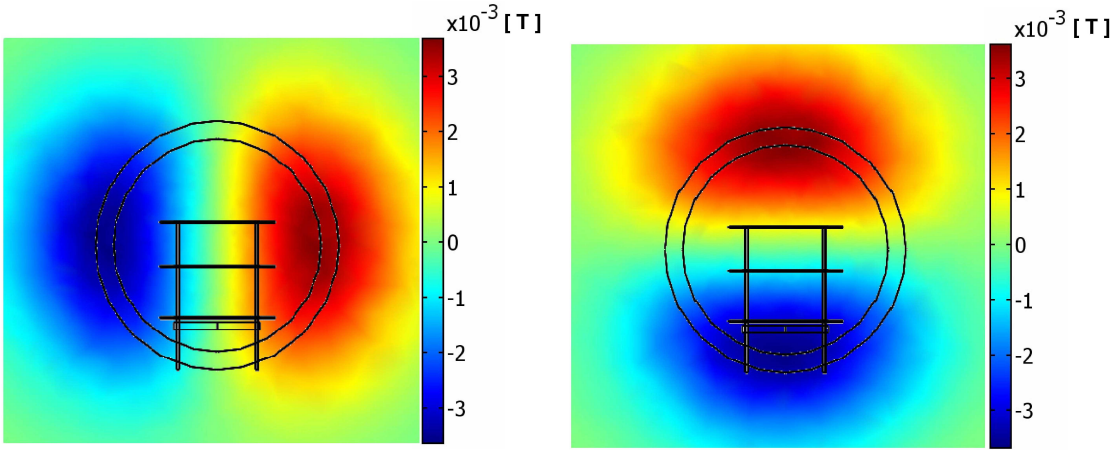

(a) (b)

Fig. 5.12: Calculated magnetic field in the vicinity of the detection MOT. a) y component of the magnetic field. b) z component of the magnetic field.

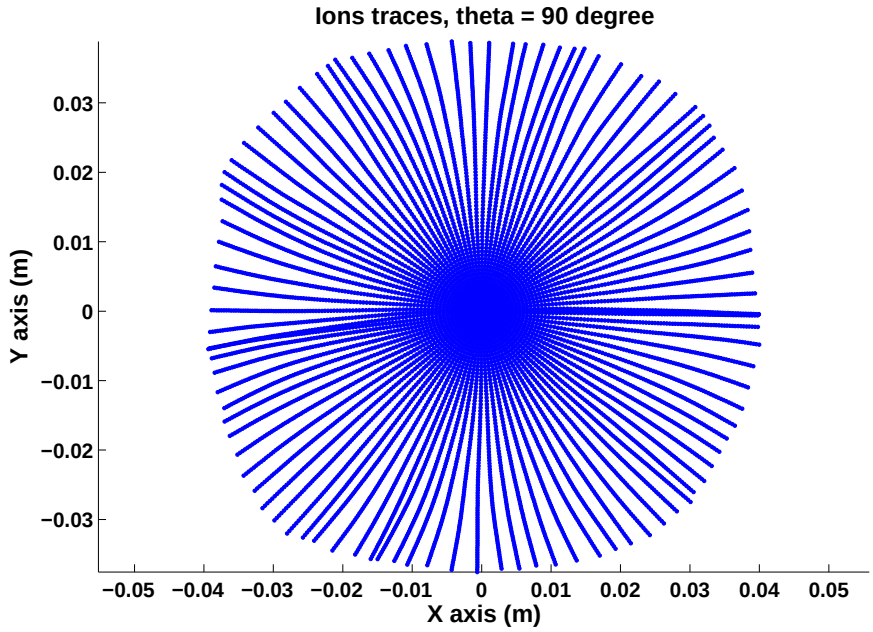

(a)

Fig. 5.13: Simulated ion traces in different directions. The initial momenta of the ions are parallel to the x-y plane. The effect of the inhomogeneities of the electric and magnetic fields on the ions causes a direction dependence of the ion impact position on the MCP.

TABLE 5.1: Modules used in the MCP readout electronics (see Fig. 5.14).

Abbr.	Module	Brand	Abbr.	Module	Brand
AO	AND-OR	L18 Univ. HD	VT	TDC	Lecroy1176
LS	Linear Scaler	Lecroy1151N	SIS	Scaler	SIS36/38xx
NE	NIM-ECL conv.	C16 Univ. HD	VA	NIM-ECL conv.	CaenV538A
RCB	Trigger	CES-RCB8047	UD	Discriminator	D16 Univ. HD

5.4.1 Data Acquisition

For every event there are 9 signals which are read out from the MCP stack. The delay line anode provides 8 signals from all ends of the 4 wires (2 in each direction) and one signal is derived from the voltage divider of the MCP stack. The difference signals from each wire pair are put into an updating discriminator to give digital NIM standard signals with 50 ns width. The timing signal also is amplified and digitized. It provides a coincidence gate on all four wire difference signals (see Fig. 5.14 and 5.15). For the timing signal we use two different threshold levels. The NIM norm signals are sent into two multi-hit TDC VME modules (LC1176). The data acquisition uses the Caddie software package developed at KVI for the TRIμP experiments [Ond07b]. The Caddie communicates between the VME modules and a back-end PC and stores the data as a structured event file. The data analysis is performed using the CERN ROOT software package [Ond07b].

5.4.2 Position and Timing Resolution

An ion source made from a hot W filament coated with NaCl and which provides Na^+ ions through surface ionization is used to measure the position and timing resolution of the recoil-ion detector. This filament is mounted on a translator which allows to position the filament at the center of the detection chamber. The filament is insulated from the chamber and is elevated to the corresponding electric potential at the center of the chamber.

The data recorded with the multi-hit TDC (Lecroy1176) is analyzed to obtain the image of the filament on the MCP detector through the emitted Na^+ ions. Figure 5.16 shows the resulting picture. The Lecroy1176 module has 1 ns timing resolution which is reflected in figure 5.17, where the sum of the times from both ends of the wires on each direction presents the total length of the wires in x and y direction.

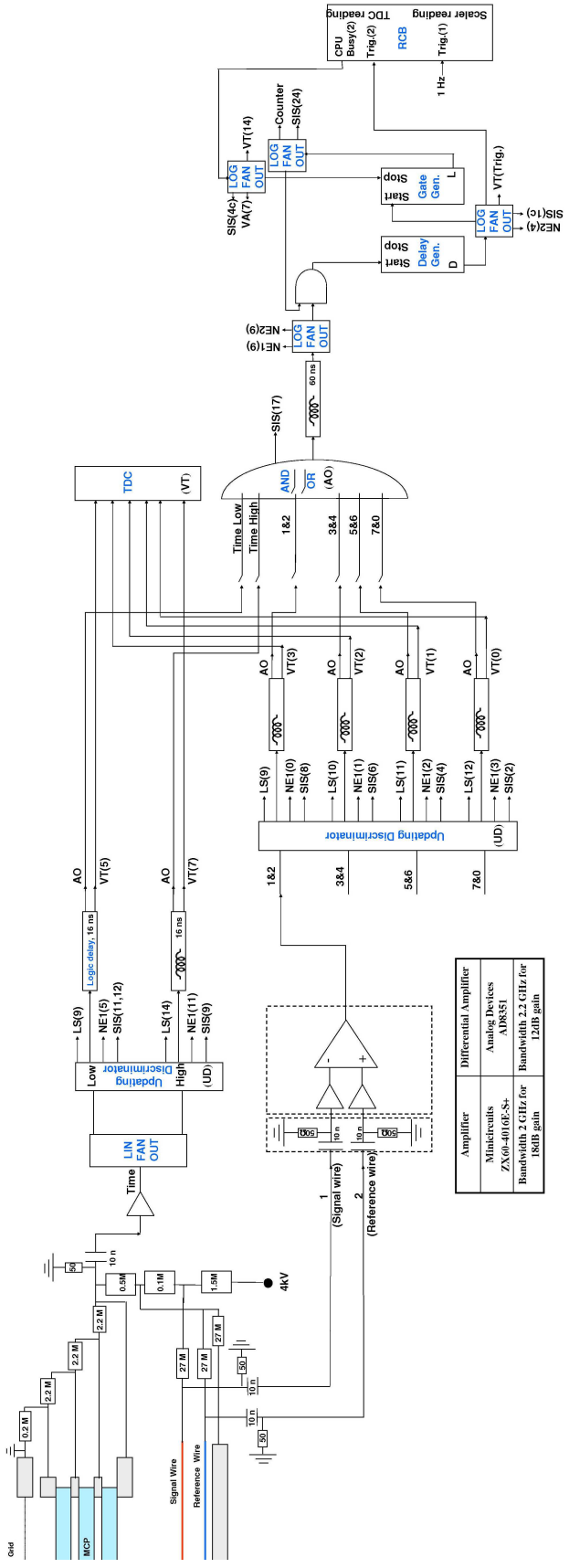

Fig. 5.14: Signals from each end of the pair of wires of the delay line anode are first individually amplified and then a pair is differentially amplified to subtract the common noise on the wires and extract the signal. The differentially amplified signals from all four ends of the delay line wire pairs are digitized in an updating discriminator module which distributes the digital signals to a multi-hit TDC and a coincidence trigger logic. The timing signal derived from the voltage divider of the MCP is amplified and then digitized in an updating discriminator module with two different thresholds. Modules used in the setup are listed in the table 5.1.

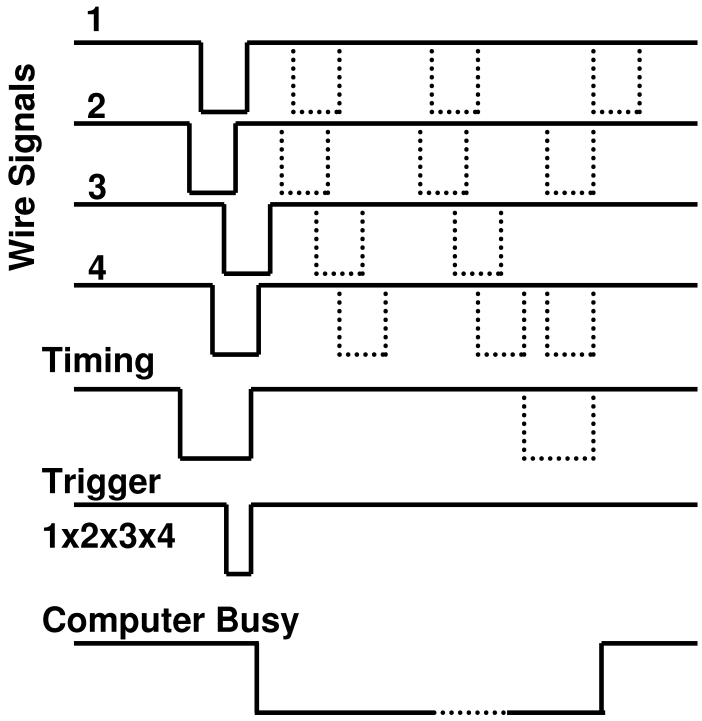

FIG. 5.15: The timing diagram of the reaction microscope event triggering. During the computer busy time, all the incoming events are not taken.

In a second test, a MOT cloud of natural Na was loaded at the center of the detection chamber. There are photo-associative ionization processes which produce slow molecular ions. In particular collision of two excited Na atoms can produce a molecular ion at negligible kinetic energy [Kir82, Kno06]. This process has been used to calibrate reaction microscopes before. The slow ions are accelerated in the electric field to an energy of 5 keV and projected onto the MCP. Figure 5.18 shows the events recorded on the MCP. The MOT cloud position is off center by a few millimeters which means either the MOT was not in the center of the chamber or the reaction microscope is not well aligned with the geometrical axis of the vacuum chamber.

By reducing the electric field one can increase the size of the image of the MOT in such a way that it covers the full sensitive MCP area. The ionization processes are very slow. The data (see Fig. 5.18) taken during $\sim$5 hours allows nevertheless to extract a position resolution of the MCP system of 1.5(0.5) mm. The position resolution obtained by two independent methods agrees very well. This resolution is sufficient for the planned measurements of the coefficient "a" in nuclear β-decay.

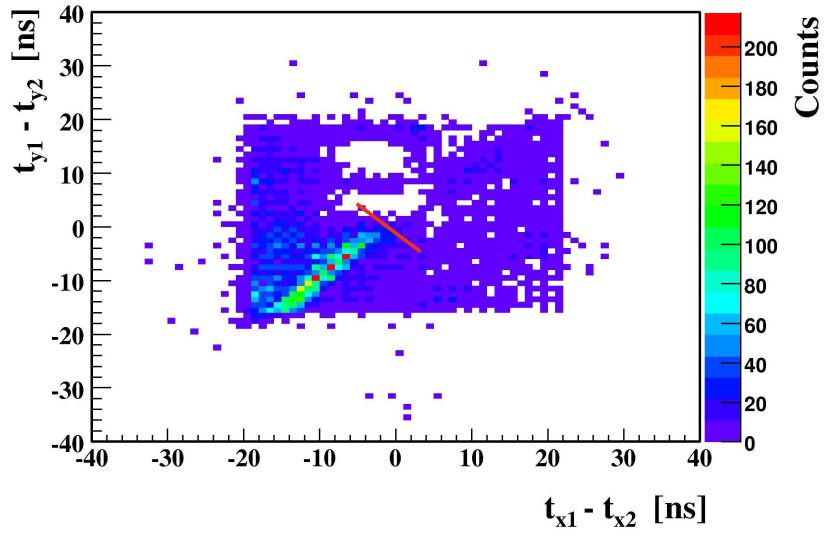

(a)

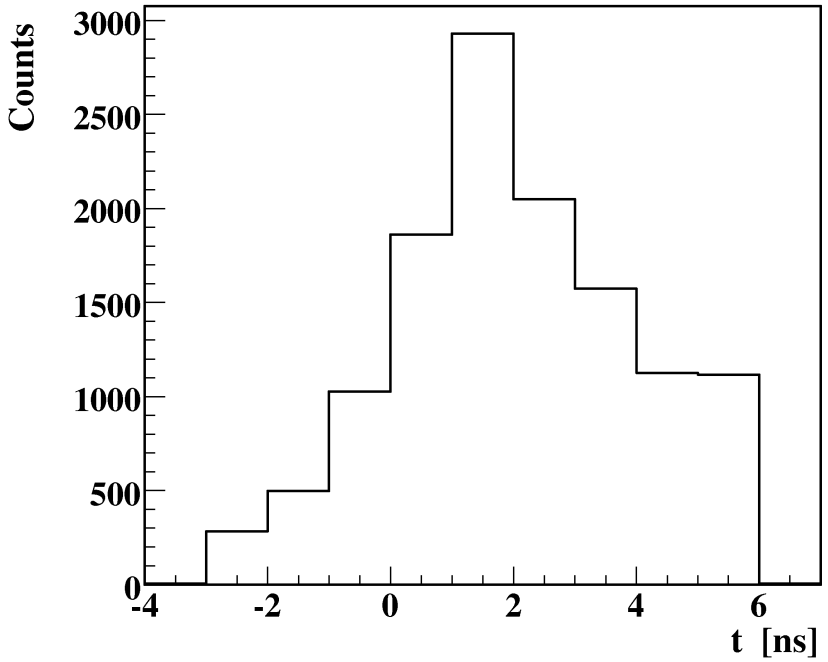

(b)

Fig. 5.16: a) The event distribution on the MCP plates produced by a hot filament close to the center of the chamber. 2 ns on each axes corresponds to 1 mm on the MCP detector. b) The projection of the peak on an axis orthogonal to the filament (indicated by a red line in (a)) shows a position resolution of about 1.5 mm (FWHM).

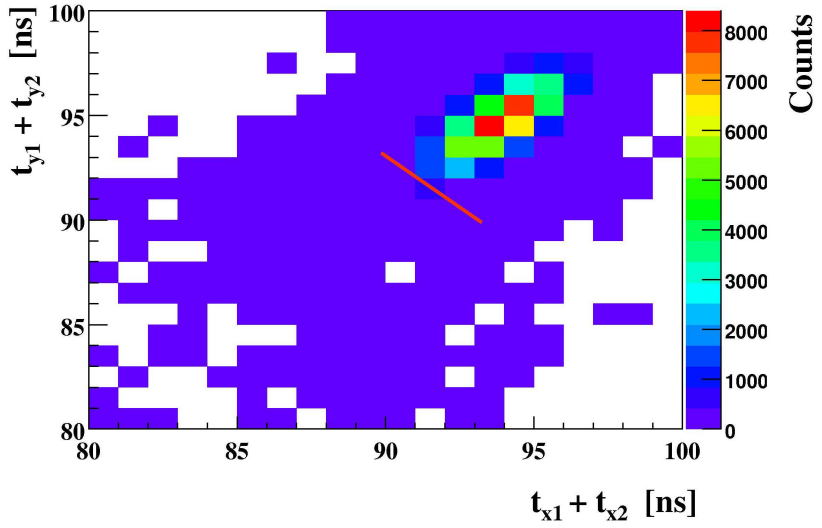

(a)

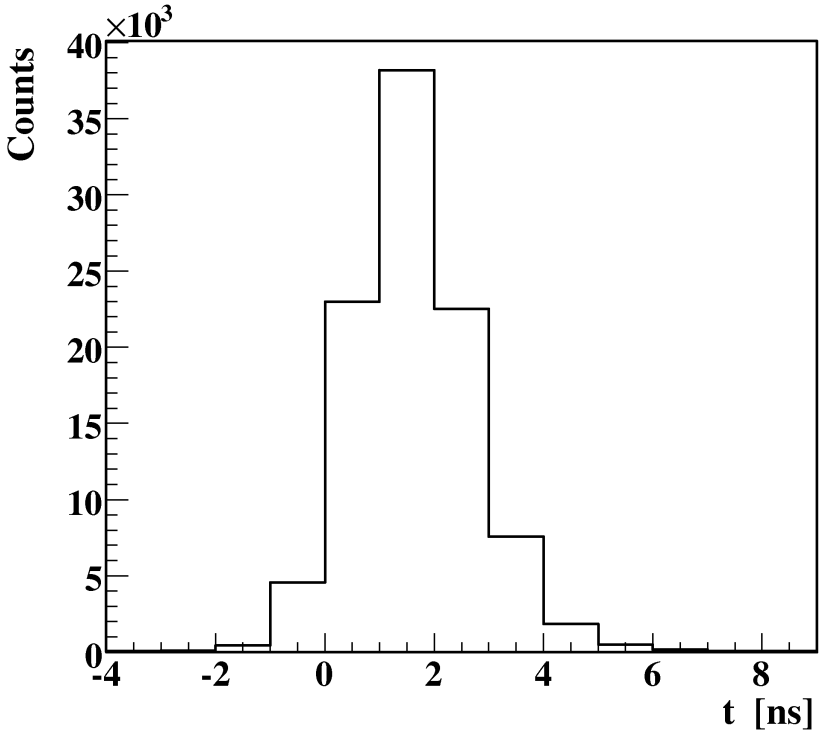

(b)

FIG. 5.17: a) The sum of the times from both ends of the wires on each direction shows the time corresponding to the total length of the wires. The width of this distribution is about 2 ns. b) A projection of the peak on a $-45°$ axis (indicated by a red line in (a)). The full width at half maximum of the signal is about 3 ns which corresponds to position resolution of 1.5(0.5) mm.

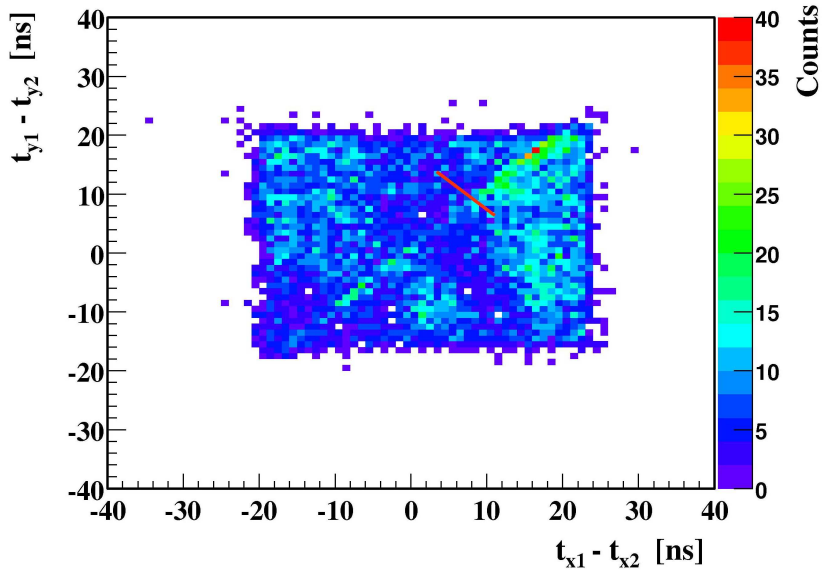

(a)

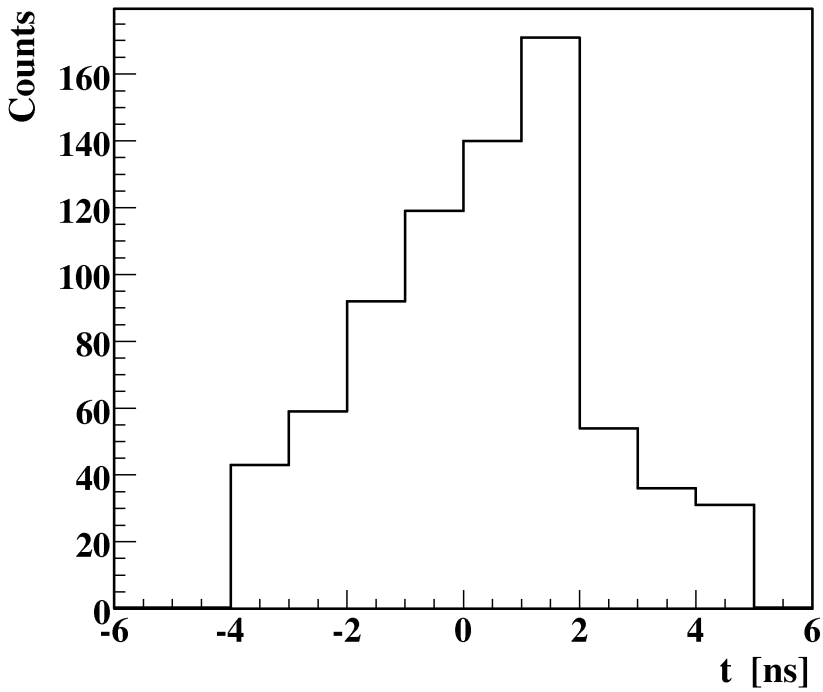

(b)

Fig. 5.18: a) The event distribution on the MCP plates produced by a MOT cloud close to the center of the chamber. 2 ns on each axes corresponds to 1 mm on the MCP detector. b) A projection of the peak on a $-45°$ axis (indicated by a red line in (a)). The width (FWHM) of the MOT cloud is about 2 mm which is the convolution of the MCP position resolution and the size of the MOT cloud.

5.5 Conclusion

A reaction microscope has been designed, fully simulated, constructed and its components have been tested. It fulfills the required performance for the foreseen β-ν asymmetry measurements. In particular,

a) it has the capability to collect the recoil-ions from nuclear β-decays in a MOT by a sufficiently strong electric field of up to 2 kV/cm.

b) it has position sensitivity on its MCP detector to resolve the full kinematics of the recoil-ions. This will provide access to the most sensitive observables in a β-decay analysis.

c) its position resolution of 1.5(0.5) mm and its timing resolution of 1 ns are limited by the data acquisition electronics, which could be improved, if needed.

A calibration with an open radioactive source is recommended to identify the position sensitivity of the detector response.